



UNIVERSIDAD  
DE ANTIOQUIA  
1803



# USE OF IRON OXYHYDROXIDES AS WATER DECONTAMINANTS: THE CASE OF AKAGANEITE

K.E. García Téllez, V. Villacorta, A. Valencia Álvarez, D.Y. Gómez Giraldo, J.-M. Greneche, C.A. Barrero Meneses.



**International Symposium  
on the Industrial Applications of the Mössbauer Effect**  
Palacký University Olomouc, September 11–16, 2022

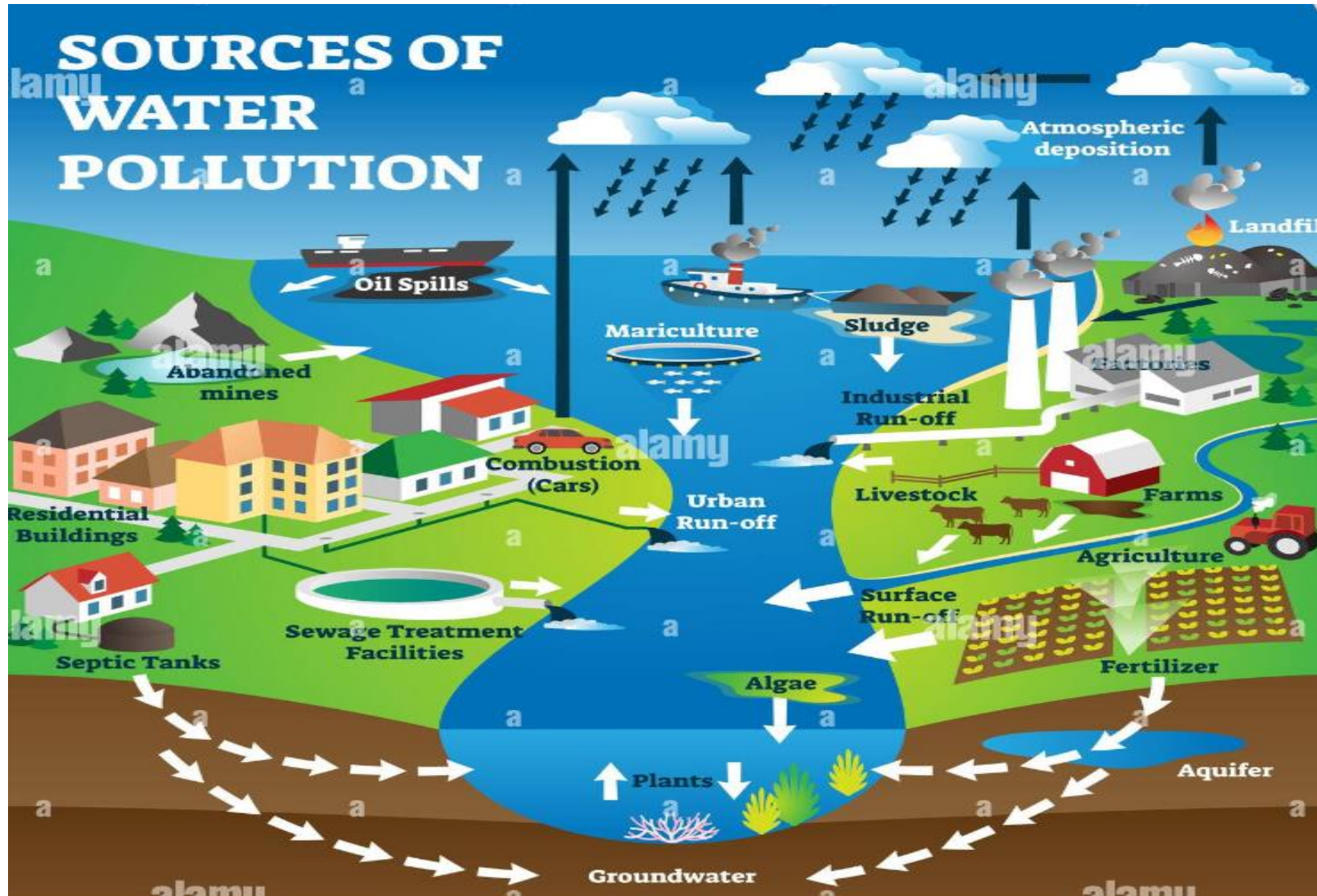
# Motivation



## SUSTAINABLE DEVELOPMENT GOALS

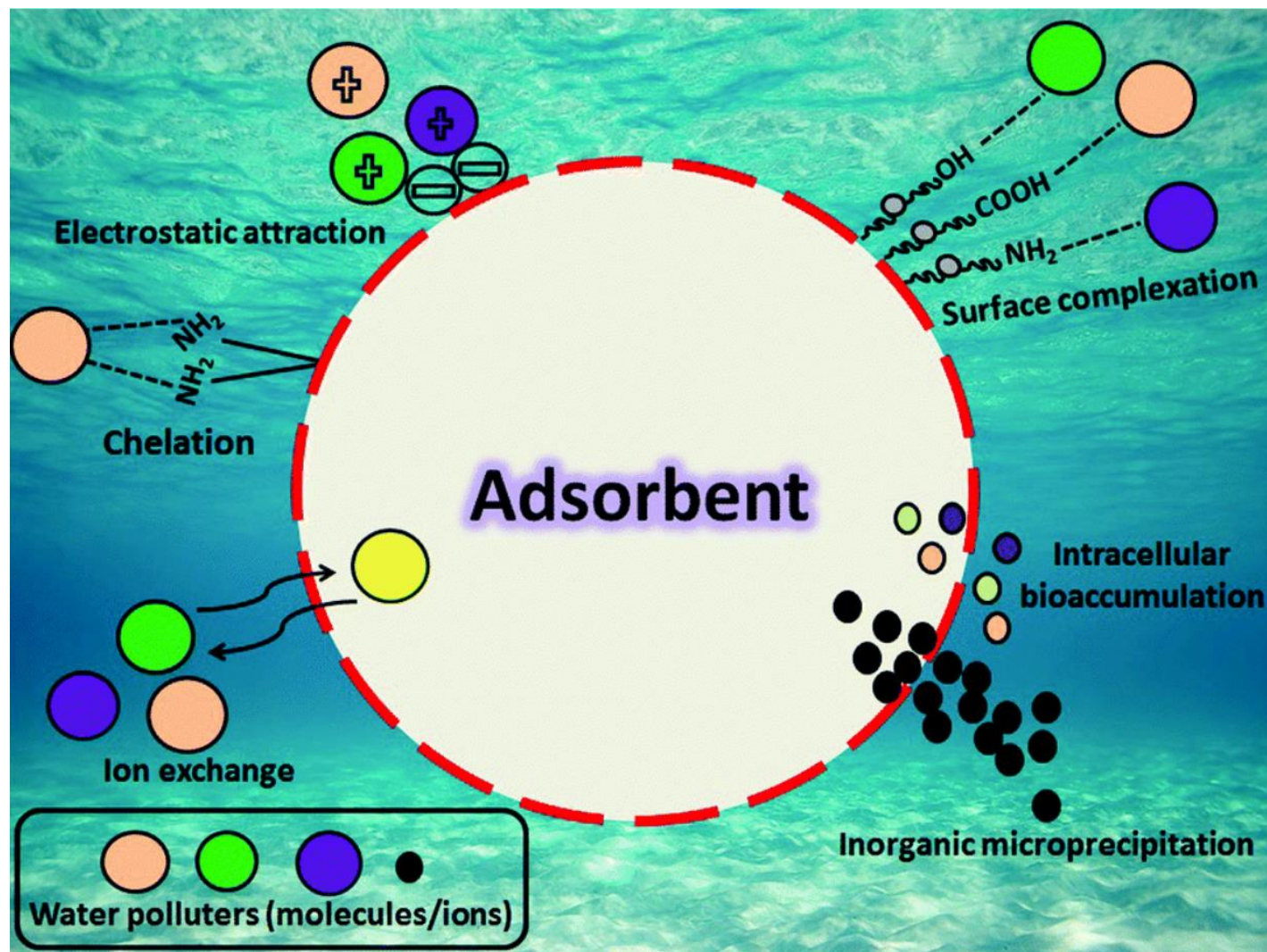


# Motivation



<https://www.alamy.com/sources-of-water-pollution>

# Motivation



# Motivation

The most commonly used iron oxyhydroxides and oxides for adsorption are ferrihydrite, goethite, ferroxhyte, hematite, and magnetite. Comparatively, akageneite has been less employed, in spite their unique properties for the efficient removal of water pollutants.

# Akaganeite

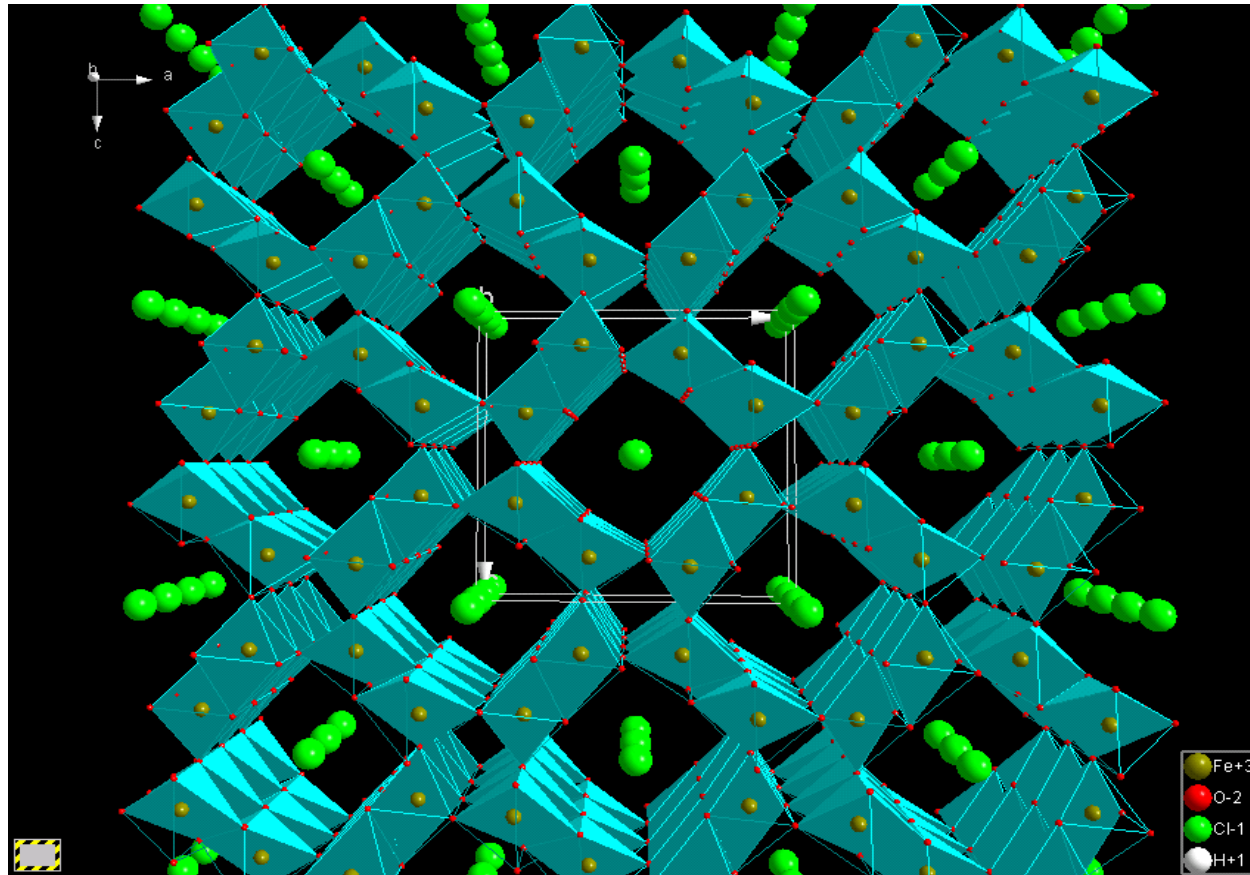
- Named after the Akagane mine, Iwate Prefecture, in Japan.
- Discovered as a mineral and named akaganeite by Dr. Matsuo Nambu of Sendai University, Japan.

*A.L. Mackay, Mineral. Mag. 33 (1962) 270.*

- $\beta$  polymorph of FeOOH.
- Iron oxyhydroxide commonly found in Cl<sup>-</sup> rich environments.

# CRYSTAL STRUCTURE

- ▶ Double chains of edge sharing  $\text{Fe}^{3+}$ -(O,OH) octahedra.
- ▶ Adjacent double chains share corners forming channels.



# I. SYNTHESIS OF AKAGANEITES IN PRESENCE OF CATIONS

The synthesis in presence of different cations and anions has been used:

- (i) for modifying physico-chemical properties (morphology, particle size, dimensionality, porosity, crystalline structure, thermal stability and surface properties)
- (ii) to enhance the performance for different applications.

## Some literature review:

➤ Akaganeite can incorporate in the structure much less than 0.06 mol.mol<sup>-1</sup> of Cr, Mn, Ni, and Zn, but up to 0.06 and 0.04 mol.mol<sup>-1</sup> of Cu and Si, respectively.

*R.M. Cornell , U. Schwertman. The Iron Oxides. 2nd, Ed.; Wiley-VCH Verlag GmbH & Co. KGaA, 2003.*

➤ β-FeOOH were synthesized from aqueous FeCl<sub>3</sub> solutions in presence of Ti(IV), Cr(III), Cu(II) and Ni(II). Ti(IV)-sulfates drastically affected the crystallization and growth of the particles.





*T. Ishikawa et al. Corros. Sci. 43 (2001) 1727; K. Garcia et al. Mater. Chem. Phys. 112 (2008) 120.*





Cite this: *CrystEngComm*, 2019, 21, 7155

## Influences of As(v), Sb(III), and Hg(II) ions on the nucleation and growth of akaganeite†

Verónica Villacorta, \*<sup>a</sup> Karen Edilma García, <sup>a</sup>  
Jean-Marc Greneche <sup>b</sup> and César Augusto Barrero <sup>a</sup>

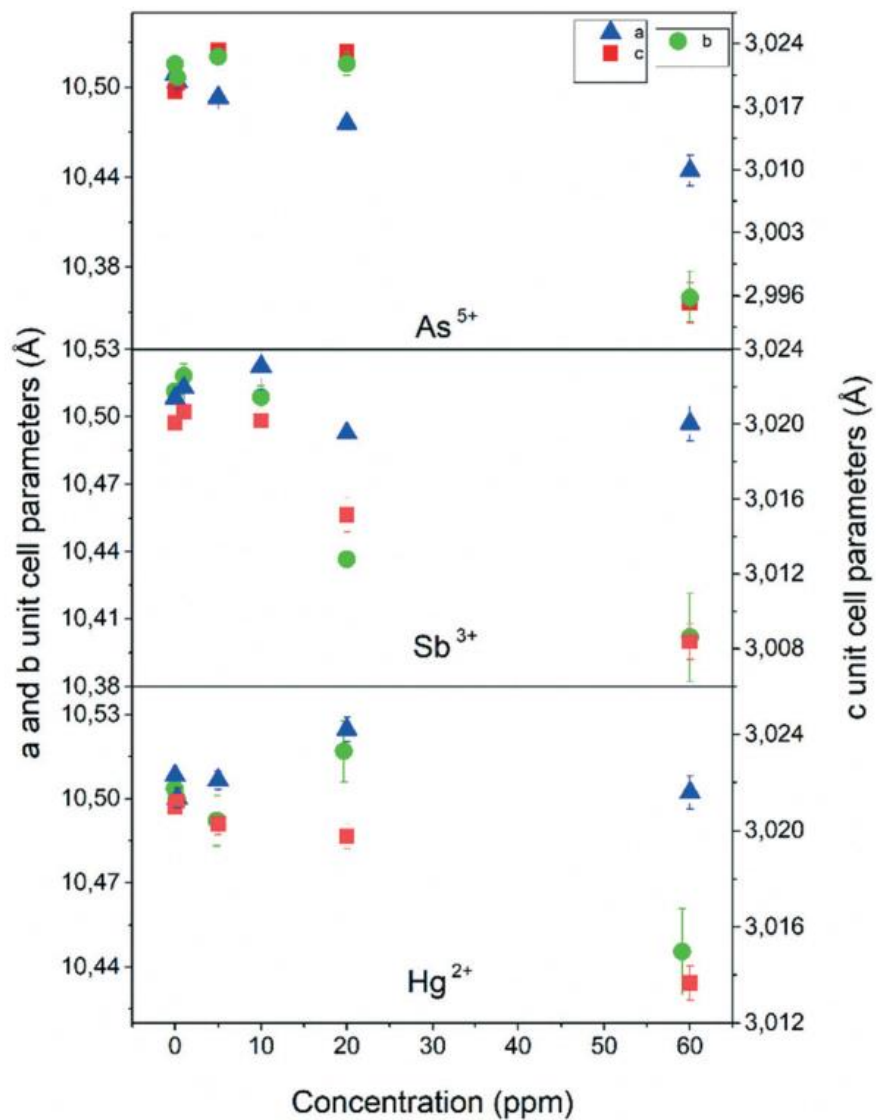
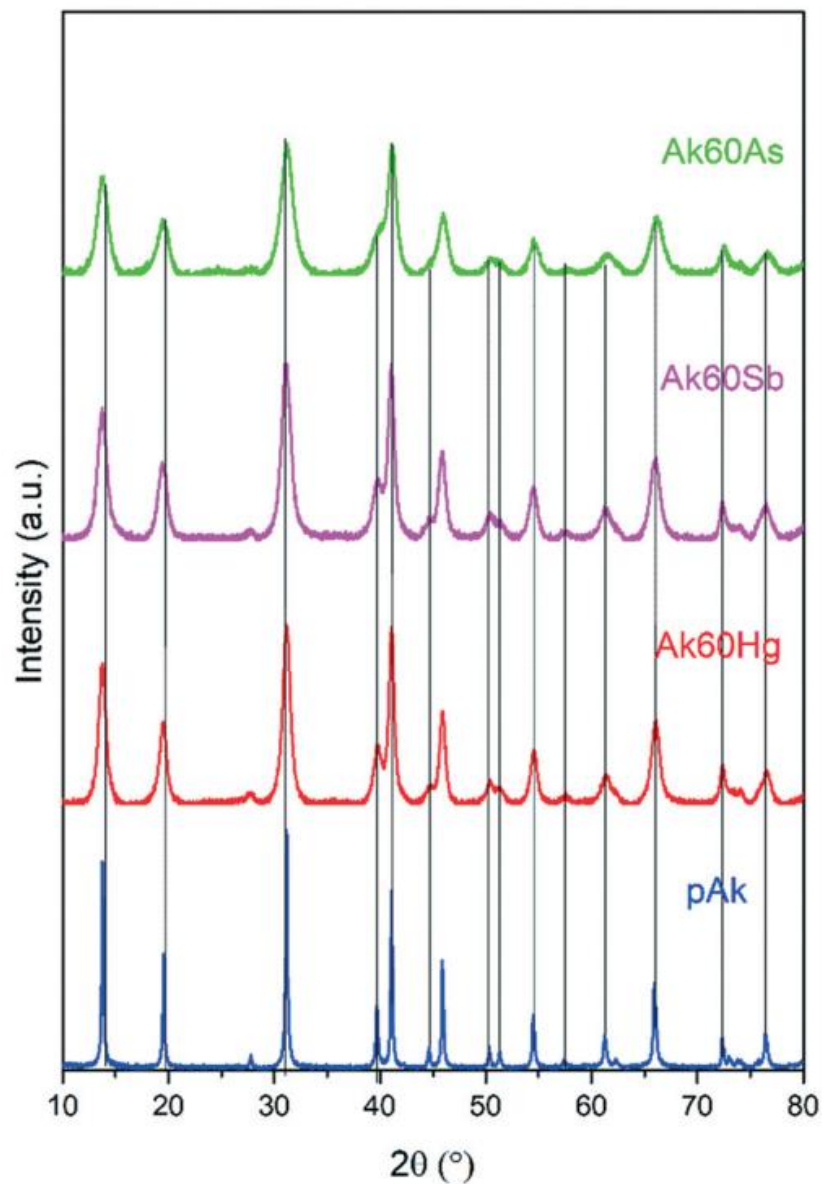
The physico-chemical properties of akaganeite are known to be modified when formed in the presence of ions, but there are no reports on these effects for arsenic, antimony and mercury. In this work, akaganeites are precipitated *via* hydrolysis of FeCl<sub>3</sub> solutions in the absence and in the presence of varying concentrations of As<sup>5+</sup>, Sb<sup>3+</sup> and Hg<sup>2+</sup>. All co-precipitated akaganeites exhibit an acicular morphology, and the increase of ion concentration greatly reduces the particle sizes and induces a transformation from nano-structured powders to nanoparticle morphologies. The variation of the mean crystallite size *versus* ion concentration is fitted to an exponential function, and the derived parameters suggest that the energy for particle growth is greater for akaganeite co-precipitated with As<sup>5+</sup>. The analysis of infrared, Raman and Mössbauer spectra suggests the replacement of OH⋯Cl groups by ionic species located at the surface and tunnel sites. The 77 K hyperfine data suggest that the iron ions in the vicinity of unoccupied chloride sites and on the surface are the most affected ones. One can unambiguously conclude that these ions do not replace iron in the lattice but are adsorbed at the surface and possibly to tunnel sites as ionic species during nucleation and growth of the particles, altering the surface tension of the nucleus and also the growth energy.

Received 25th August 2019,  
Accepted 15th October 2019

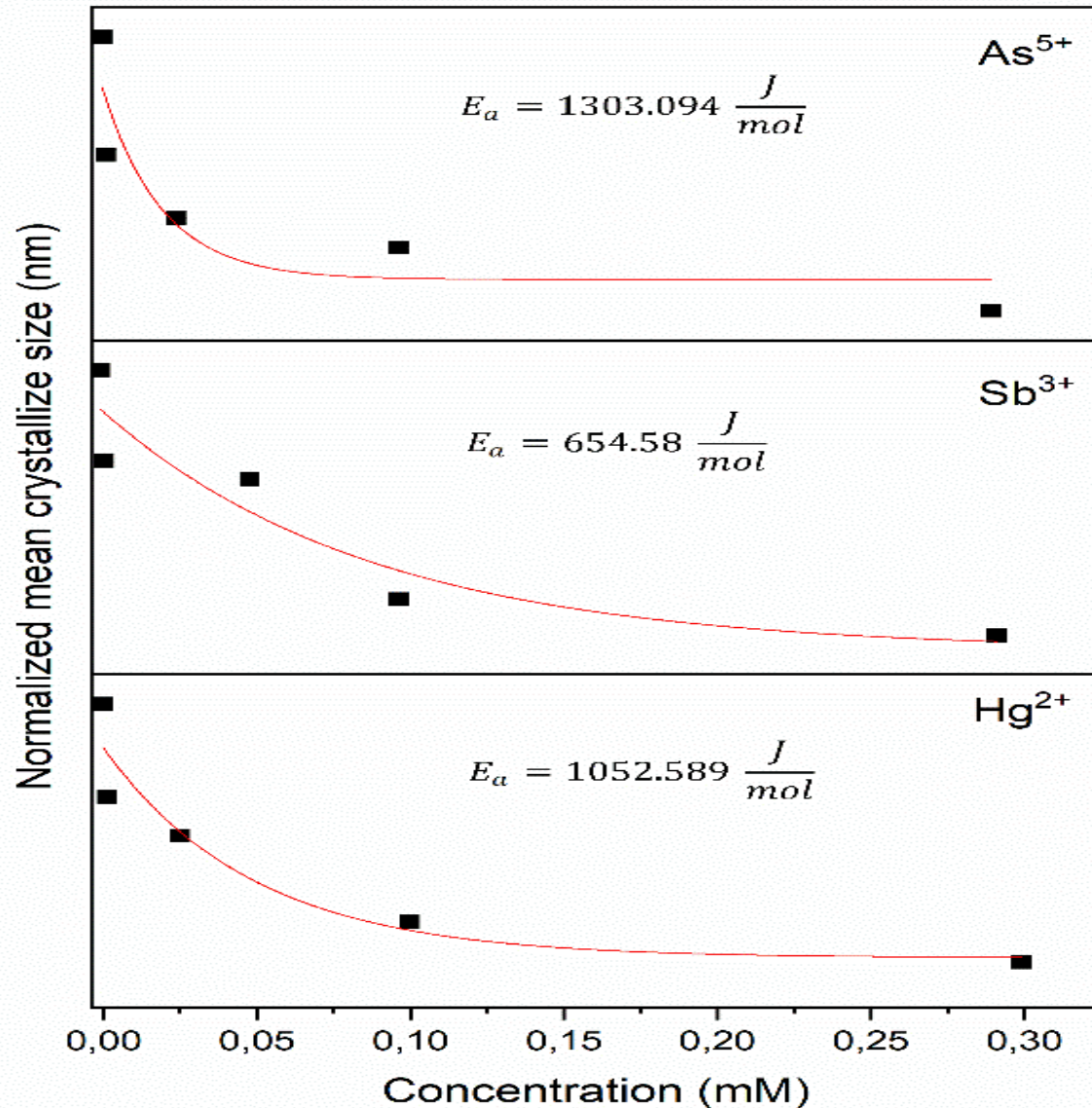
DOI: 10.1039/c9ce01345h

[rsc.li/crystengcomm](http://rsc.li/crystengcomm)

# XRD: Synthesis in presence of As, Sb and Hg

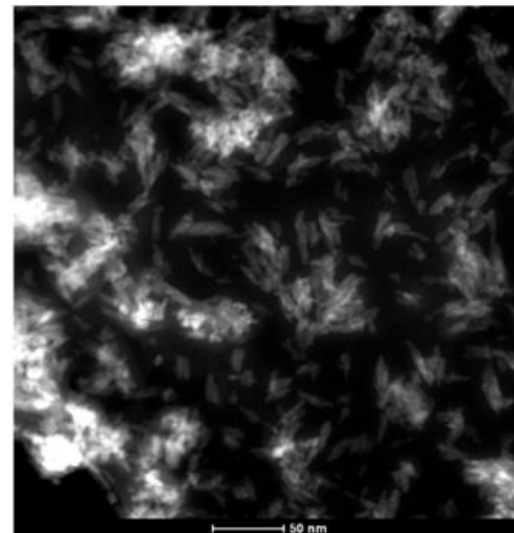
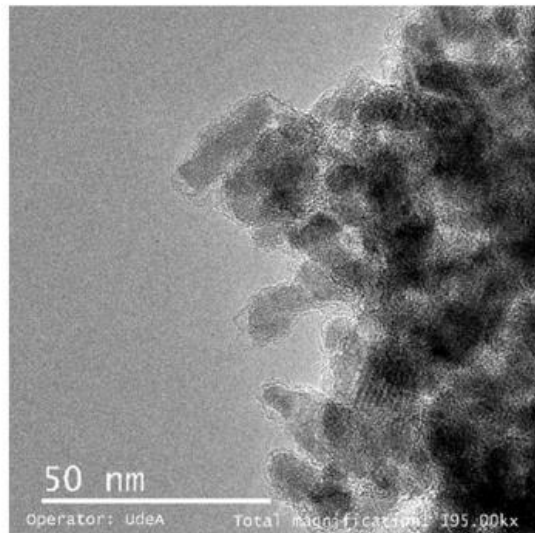
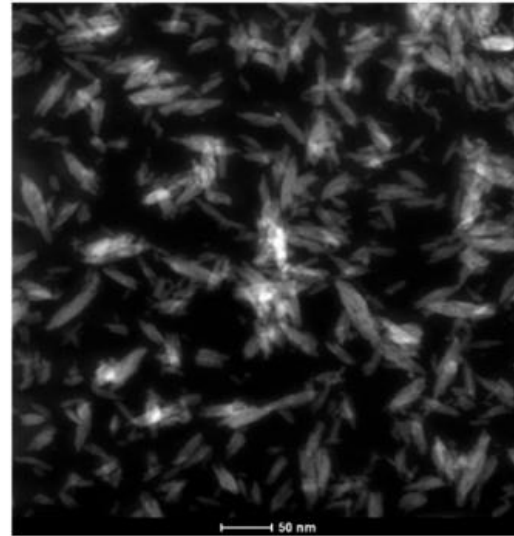
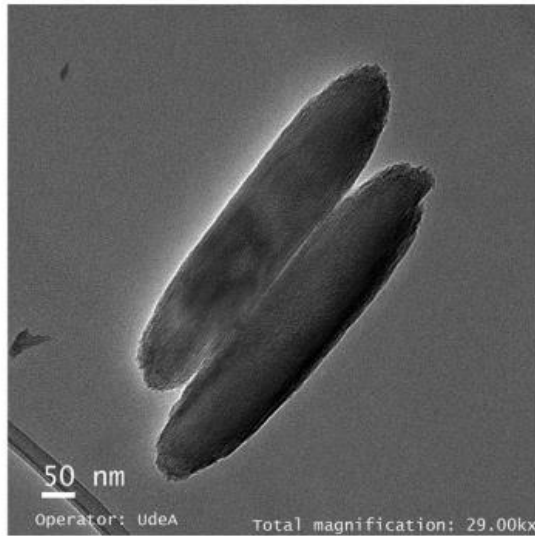


## XRD: Synthesis in presence of As, Sb and Hg



$$\frac{D[x]}{D_0} = A + B \exp(-C[x])$$

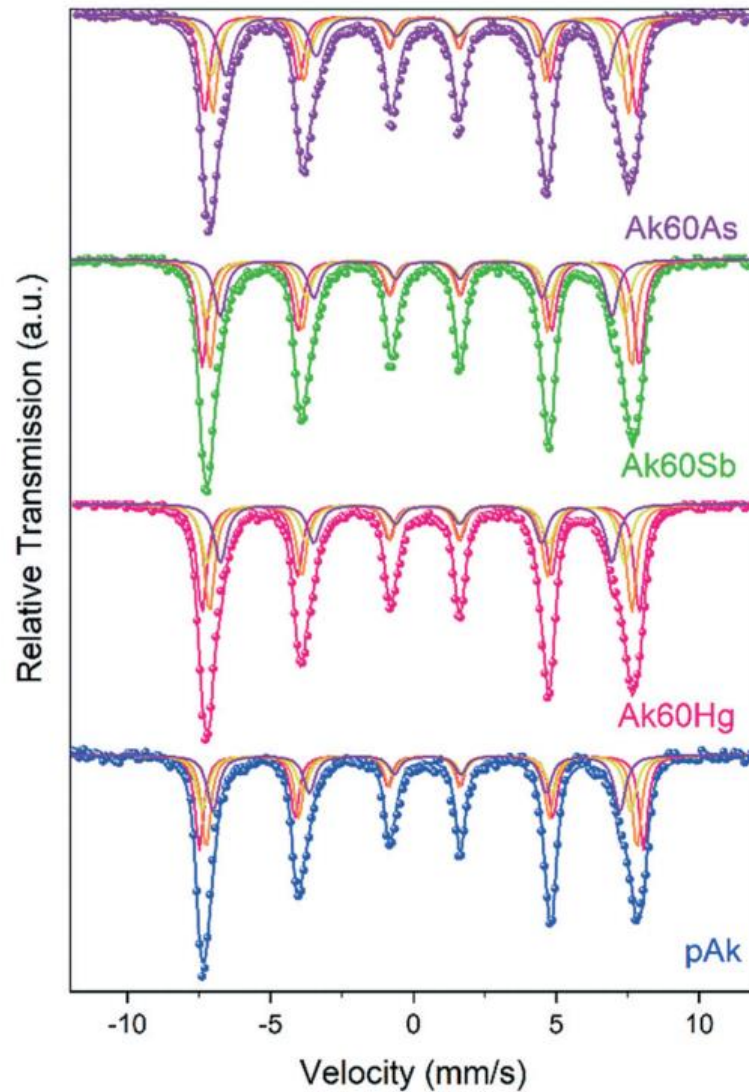
## TEM: Synthesis in presence of As, Sb and Hg



Average particles lengths, widths and aspect ratio, AR, of pure akaganeite and akaganeites co-precipitated with the ions at 60 ppm concentration (TEM analysis).

Sample	Length (nm)	Width (nm)	Aspect ratio (AR = Width/Length)
Pak	503±39	107±12	0.21
Ak60Hg	29±11	9±3	0.31
Ak60Sb	23±6	6±2	0.26
Ak60As	13±3	4±1	0.31

# MÖSSBAUER SPECTROSCOPY: Synthesis in presence of As, Sb and Hg



Hyperfine parameters of the 77K Mössbauer spectra for akaganeites co-precipitated with  $\text{As}^{5+}$ . Isomer shift ( $\delta$ ), quadrupolar shift ( $2\varepsilon$ ), hyperfine field ( $B_{\text{hf}}$ ) and relative absorption area (A).

	S1				S2				S3				S4			
Sample	$\delta$ (mm/s)	$2\varepsilon$ (mm/s)	B (T)	Area (%) $\pm 2$	$\delta$ (mm/s)	$2\varepsilon$ (mm/s)	B (T)	Area (%) $\pm 2$	$\delta$ (mm/s)	$2\varepsilon$ (mm/s)	B (T)	Area (%) $\pm 2$	$\delta$ (mm/s)	$2\varepsilon$ (mm/s)	B (T)	Area (%) $\pm 2$
pAk	0.50 $\pm 0.01$	-0.09 $\pm 0.01$	48 $\pm 0.5$	28	0.50 $\pm 0.01$	-0.09 $\pm 0.01$	46.5 $\pm 0.6$	28	0.47 $\pm 0.01$	-0.39 $\pm 0.02$	46.3 $\pm 2.0$	22	0.47 $\pm 0.01$	-0.39 $\pm 0.02$	44.0 $\pm 1.2$	22
Ak5As	0.49 $\pm 0.01$	-0.09 $\pm 0.01$	48.0 $\pm 0.5$	27	0.49 $\pm 0.01$	-0.09 $\pm 0.01$	46.7 $\pm 0.6$	27	0.46 $\pm 0.01$	-0.39 $\pm 0.02$	46.3 $\pm 1.9$	23	0.46 $\pm 0.01$	-0.39 $\pm 0.02$	44.1 $\pm 1.0$	23
Ak20As	0.49 $\pm 0.01$	-0.11 $\pm 0.01$	47.9 $\pm 0.5$	30	0.49 $\pm 0.01$	-0.11 $\pm 0.01$	46.4 $\pm 0.5$	30	0.46 $\pm 0.01$	-0.41 $\pm 0.02$	46.0 $\pm 1.6$	20	0.46 $\pm 0.01$	-0.41 $\pm 0.02$	43.6 $\pm 0.9$	20
Ak60As	0.48 $\pm 0.01$	-0.14 $\pm 0.01$	46.7 $\pm 0.7$	27	0.48 $\pm 0.01$	-0.14 $\pm 0.01$	44.9 $\pm 0.8$	27	0.45 $\pm 0.01$	-0.28 $\pm 0.02$	44.2 $\pm 2.5$	23	0.45 $\pm 0.01$	-0.28 $\pm 0.02$	41.1 $\pm 1.5$	23

77K hyperfine data suggested that the iron ions at the vicinity of unoccupied chloride sites are the most affected ones.

# Main findings (Part I)

As, Sb and Hg ions did not replace Fe in the lattice but were adsorbed at the surface and possibly to tunnel sites as ionic species during nucleation and growth of the particles, altering the surface tension of the nucleus and also the growth energy.

The co-precipitated akaganeites exhibited acicular morphology, and the increment of As, Sb and Hg concentration greatly reduced the particle sizes.

Mössbauer spectroscopy suggested that among the irons, those at the vicinity of unoccupied chloride sites are the most affected ones.



## II. ADSORBENTS BASED ON AKAGANEITES

Akaganeite offers unique properties for the efficient removal of pollutants from aqueous solutions, such as large specific surface area, presence of tunnel sites and ample possibilities of synthesis with modified surfaces.

*E.A. Deliyanni et al. Chapter 14, G.K. Athanasios and C. Mitropoulos, Editors. Composite Nanoadsorbents. 1<sup>st</sup> edition. Elsevier. Dec. 2018.*

*J. Zhao et al. Environ. Technol. Reviews 1 (2012) 114*

*E.A. Deliyanni et al. J. Hazard. Mater. 172 (2009) 550*

### **Some literature review:**

- Two pure akaganeites with different crystallinities, specific surface areas and pores had comparable sorption loadings (Langmuir equation). Charge of the adsorber was the most important factor for adsorption of aqueous antimony and arsenic species.

*F. Kolbe et al. J. Colloid Inter. Sci. 357 (2011) 460.*

## Some literature review:

- Zr-doped  $\beta$ -FeOOH exhibited highly effective adsorption of arsenic with a capacity for As(III) and As(V) of 120 and 60mgg<sup>-1</sup> at neutral pH.

*X. Sun et al. J. Chem. Technol. Biotechnol. 88 (2013) 629*

- Akaganeite nanocrystals were used to adsorb As(V). Adsorption isotherms were fitted to Langmuir equation. The maximum load capacity was ~ 100–120 mg As(V) per g of akaganeite.

*E.A. Deliyanni et al. Chemosphere 50 (2003) 155*

- Akaganeite and surfactant modified akaganeite are very efficient adsorbers for As removal. Langmuir (isotherm) and PSO (kinetic) equations

*I. Polowczyk et al. Water Air Soil Pollut. 229 (2018) 203*

- Al<sup>3+</sup>-substituted akaganeites of different morphologies were used to adsorb As(V). Morphological characteristics are the main factor in determining the absorption properties.

*A.E. Tufo et al. J. Environ. Chem. Engin. 6 (2018) 7044*

## PAPER

Cite this: *RSC Adv.*, 2020, 10, 42688

## Removal of $\text{As}^{3+}$ , $\text{As}^{5+}$ , $\text{Sb}^{3+}$ , and $\text{Hg}^{2+}$ ions from aqueous solutions by pure and co-precipitated akaganeite nanoparticles: adsorption kinetics studies†

Verónica Villacorta,<sup>a</sup> César Augusto Barrero,<sup>a</sup> María-Belén Turrión,<sup>b</sup> Francisco Lafuente,<sup>b</sup> Jean-Marc Greneche,<sup>c</sup> and Karen Edilma García<sup>a</sup>

Adsorption kinetics models have been used to evaluate the adsorption behaviour of pollutants on different materials but there are no reports for the adsorption of  $\text{As}^{5+}$ ,  $\text{As}^{3+}$ ,  $\text{Sb}^{3+}$  and  $\text{Hg}^{2+}$  on co-precipitated akaganeite nanoparticles which were previously formed in the presence of these ions. In this research, the performance of pure and co-precipitated akaganeite nanoparticles as adsorbents of  $\text{As}^{3+}$ ,  $\text{As}^{5+}$ ,  $\text{Sb}^{3+}$  and  $\text{Hg}^{2+}$  in aqueous solutions was evaluated using the nonlinear kinetics models of Langmuir, Lagergren, Ho–McKay, Bangham, Elovich and simplified Elovich. In addition, transmission  $^{57}\text{Fe}$  Mössbauer spectrometry was used for the first time to compare the physico-chemical properties of akaganeite before and after the adsorption processes. The results showed that co-precipitated akaganeites had much better adsorption capacities than pure akaganeites. On the other hand, the  $\text{Sb}^{3+}$  and  $\text{Hg}^{2+}$  were the fastest and slowest pollutants respectively adsorbed on all akaganeites. The kinetics models that best described the experimental data for  $\text{As}^{3+}$ ,  $\text{As}^{5+}$  and  $\text{Sb}^{3+}$  were those of Elovich and simplified Elovich. For  $\text{Hg}^{2+}$ , the kinetic model that best described the experimental data was that of Bangham. The 300 K and 77 K Mössbauer spectrometry showed only slight variations in some of the hyperfine parameters for the akaganeites after adsorption.

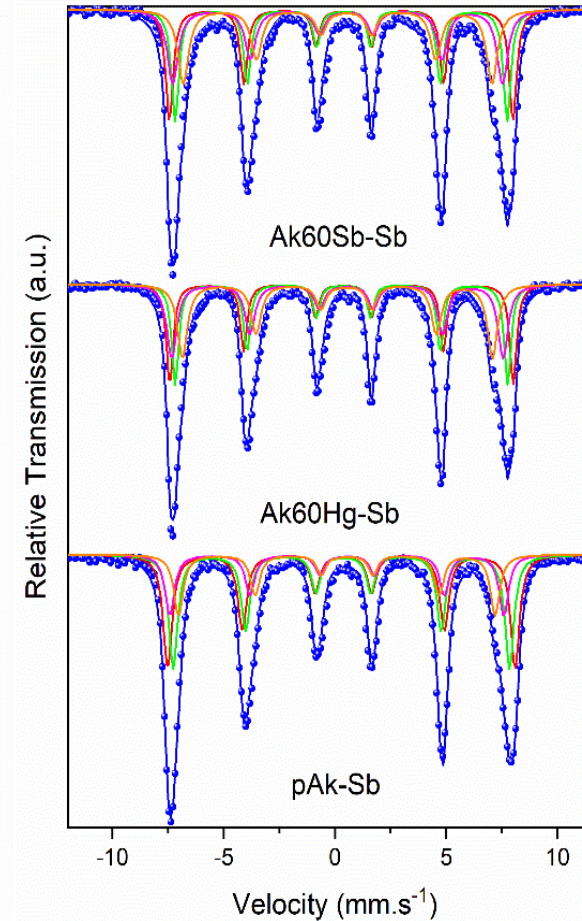
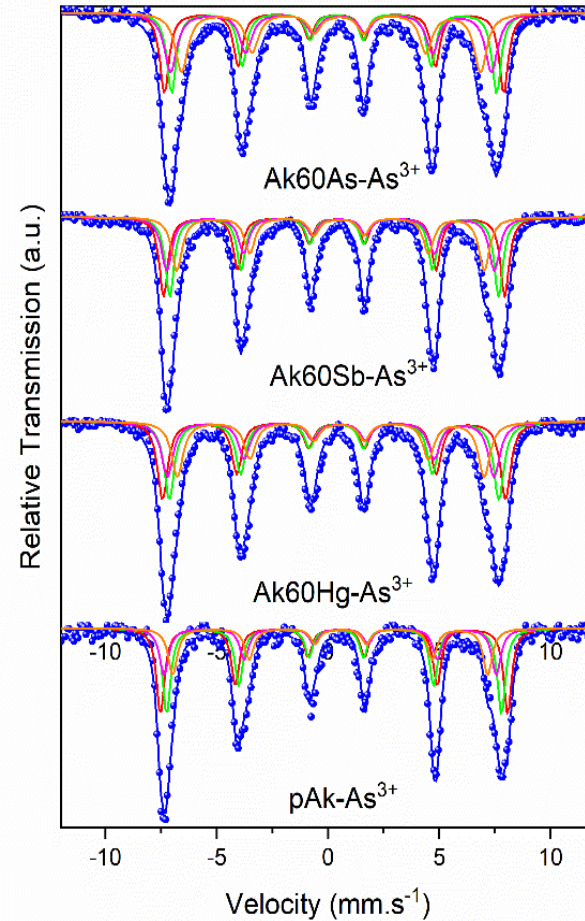
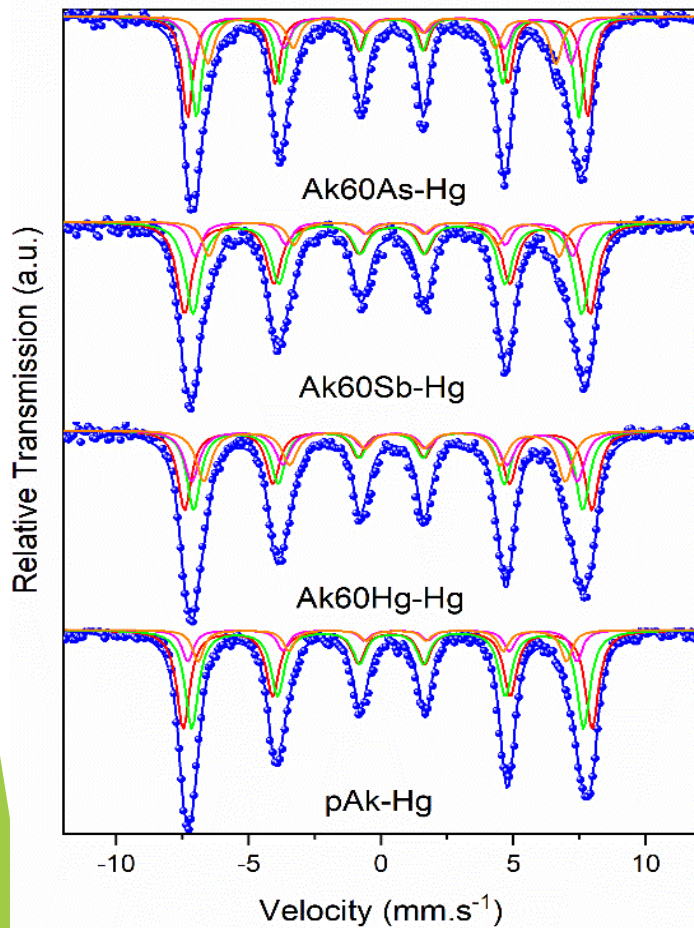
Received 21st September 2020  
Accepted 3rd November 2020

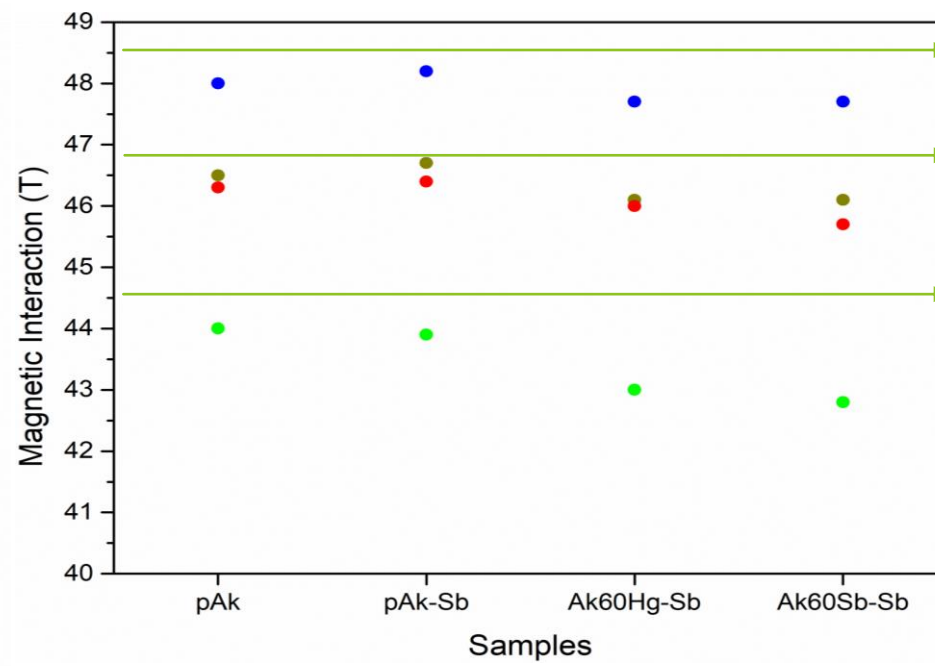
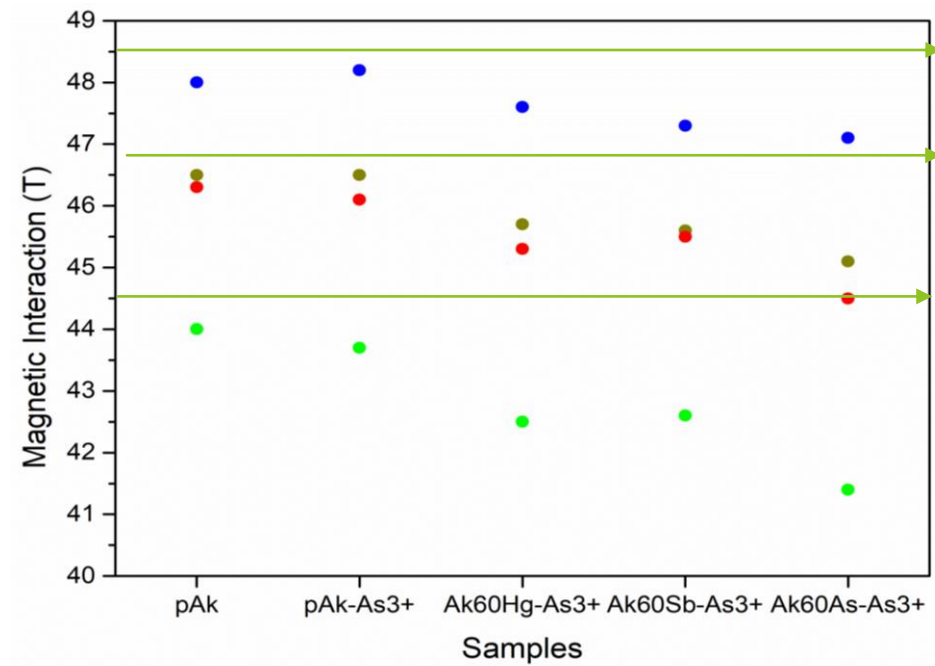
DOI: 10.1039/d0ra08075f

[rsc.li/rsc-advances](https://rsc.li/rsc-advances)

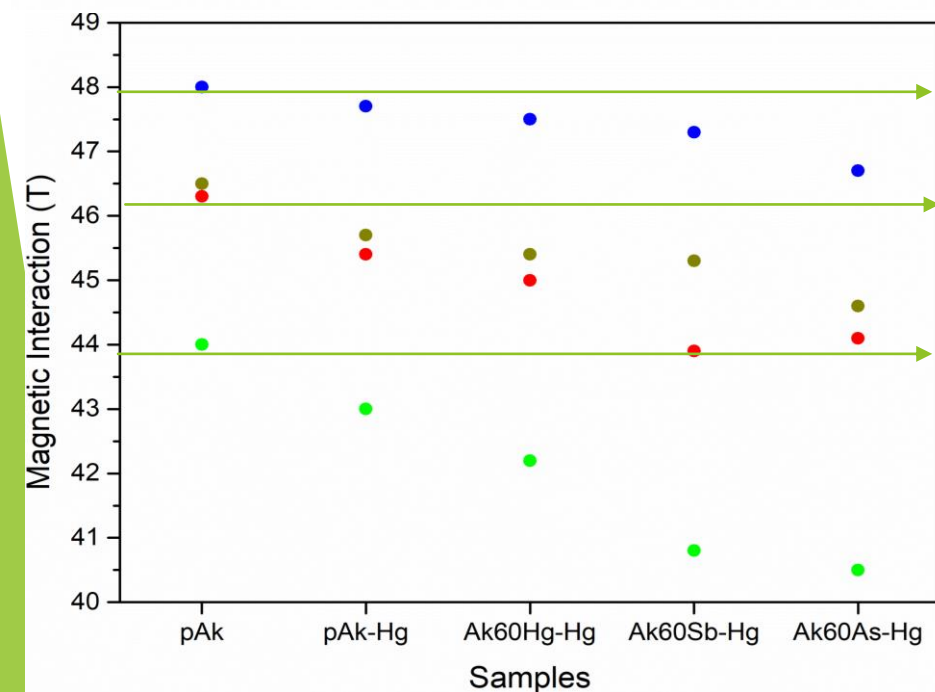
At 77K spectra adequately fitted by introducing at least four components:

**S1** (Fe1-Cl), **S2** (Fe2-Cl), **S3** (Fe1-VCl) and **S4** (Fe2-VCl).






- Magnetic interaction S1
- Magnetic interaction S2
- Magnetic interaction S3
- Magnetic interaction S4




The magnetic interactions for sites S1, S2, S3 and S4 for samples adsorbing  $\text{Hg}^{2+}$  were lower than those adsorbing  $\text{As}^{3+}$  and  $\text{Sb}^{3+}$ .

The population of p-d valence shell was affected by the molecular bonding of the iron with its neighbors, probably due to the ions adsorbed at the surface.

Many adsorptions kinetic models have been reported in the literature, but only very few of them have been used to fit the kinetic experimental data.

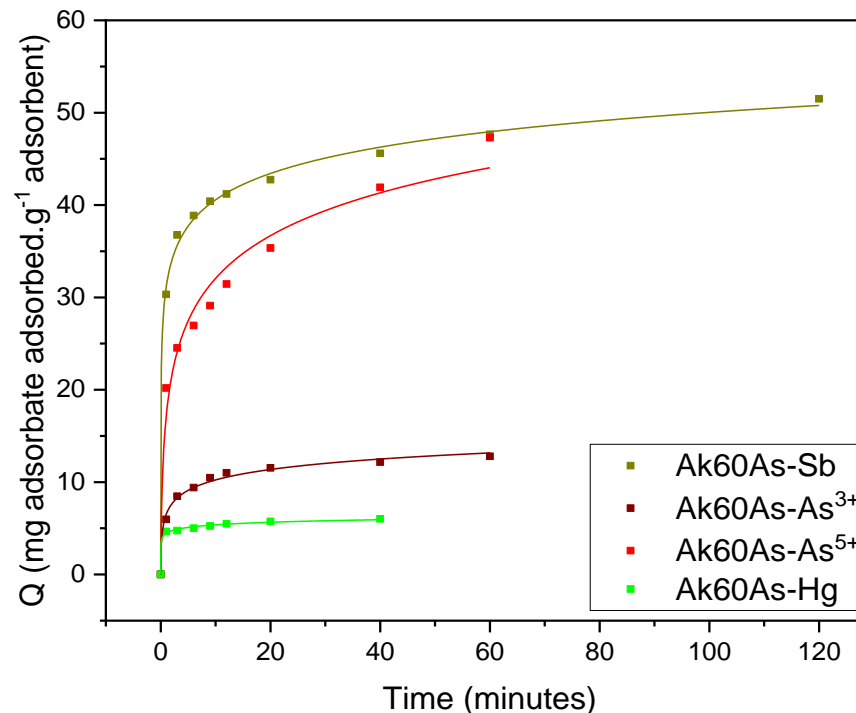
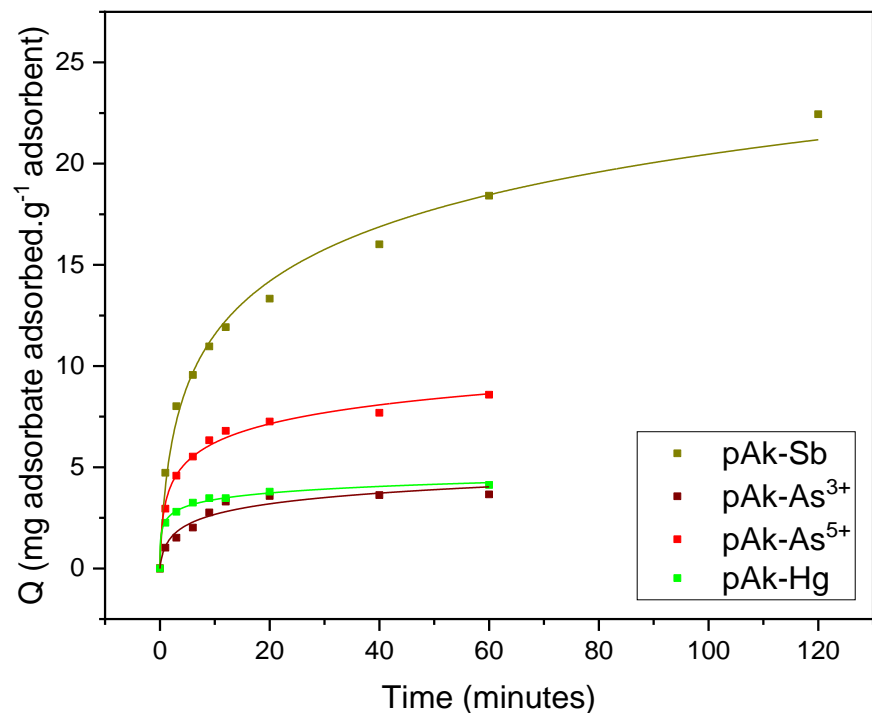


It is important to know the kinetic characteristics, because it allows a prediction of the rate of removal of contaminants using adsorbents, which is a crucial factor for the design and operation of an effective adsorption system.



In this work, 22 models have been explored and it was found that the fractal kinetic models were the ones that better described the kinetic adsorption processes.

## Adsorption kinetics of As, Sb and Hg on akaganeite



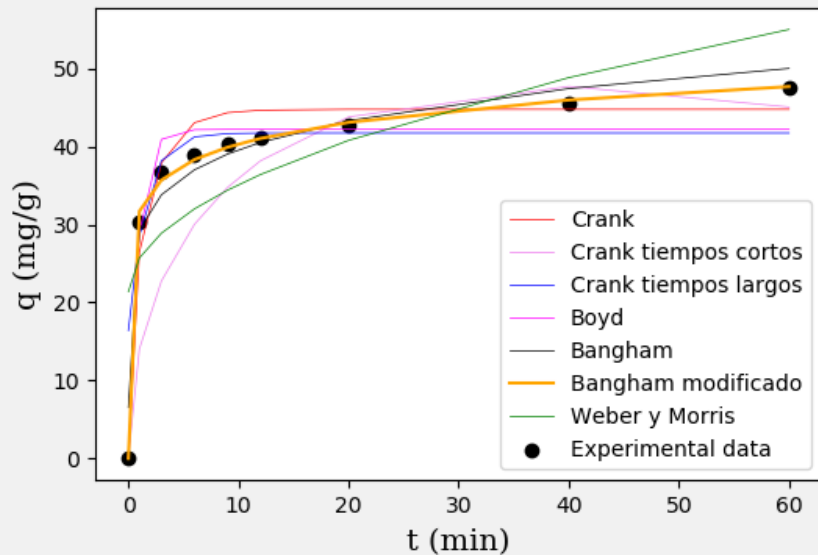
Experimental conditions: solutions of 200 mL at 40 ppm adsorbate concentration were contacted with 100 mg of adsorbents. Temperature of 25 °C. pH 3.

Nonlinear kinetic model of adsorption of Elovich

$$Q = \left(\frac{1}{\beta}\right) \ln(1 + \alpha\beta t)$$

## DIFUSION MODELS

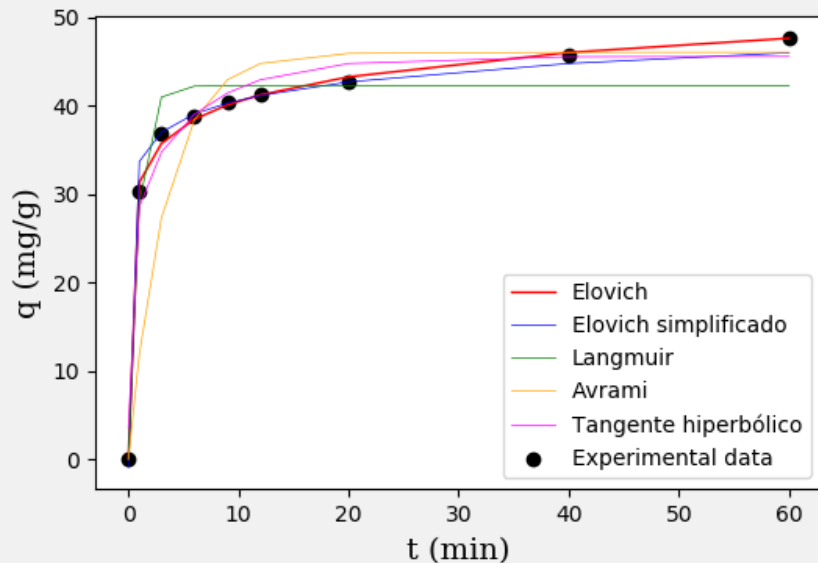
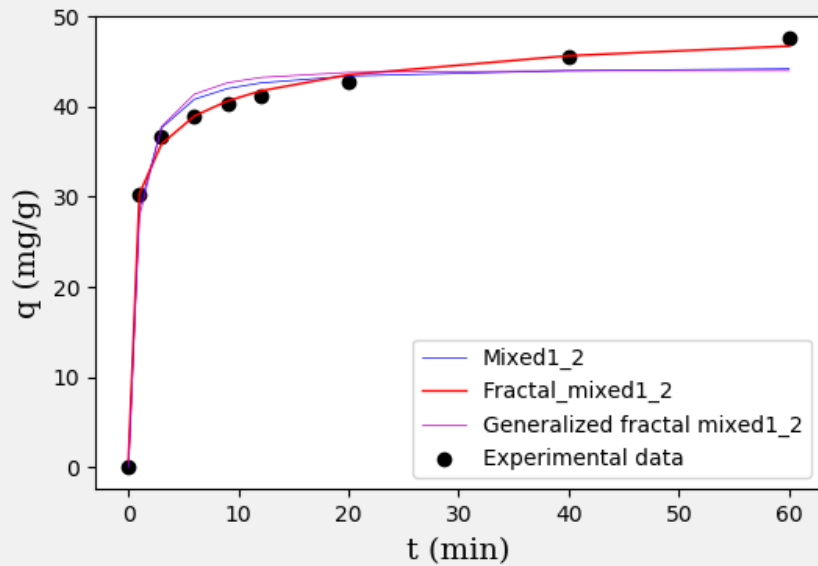
**Experimental conditions:** solutions of 200 mL at 40 ppm adsorbate ( $\text{Sb}^{3+}$ ) concentration were contacted with 100 mg of adsorbents (60 ppm  $\text{As}^{5+}$  co-precipitated akaganeite). Temperature of 25 °C. pH 3.



Model	Equation
Boyd	$q_t = q_e(1 - e^{-\frac{R}{2.303}t})$
Crank	$\frac{q_t}{q_e} = 1 - \left(\frac{6}{\pi^2}\right) \sum_{n=1}^{\infty} \left(\frac{1}{n^2}\right) \exp\left(-\frac{D_s n^2 \pi^2 t}{R^2}\right)$
Crank short times	$\frac{q_t}{q_e} = 6 \left(\frac{D_s t}{R^2}\right)^{1/2} \left[ \pi^{-1/2} - \frac{1}{2} \left(\frac{D_s t}{R^2}\right)^{1/2} \right]$
Simplified Crank short times	$q_t = 6 \left(\frac{D_s}{\pi R^2}\right)^{1/2} t^{1/2}$
Weber and Morris	$q_t = kt^{1/2} + C$
Bangham	$q_t = kt^\theta$
Modified Bangham	$q_t = kt^\theta + C$
Crank long times or Boyd	$\frac{q_t}{q_e} = 1 - \left(\frac{6}{\pi^2}\right) \exp\left(-\frac{D_s \pi^2 t}{R^2}\right)$

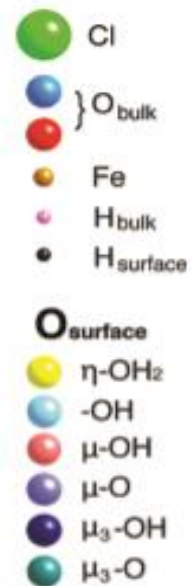
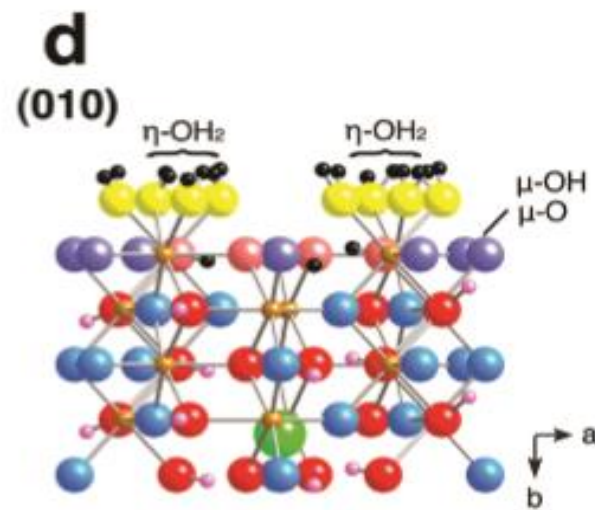
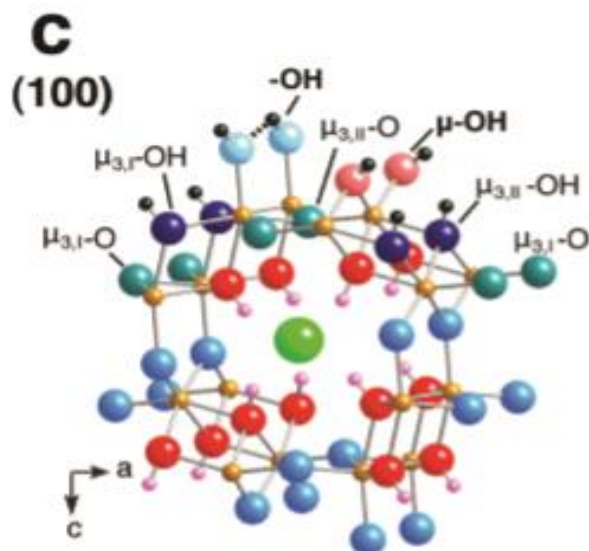
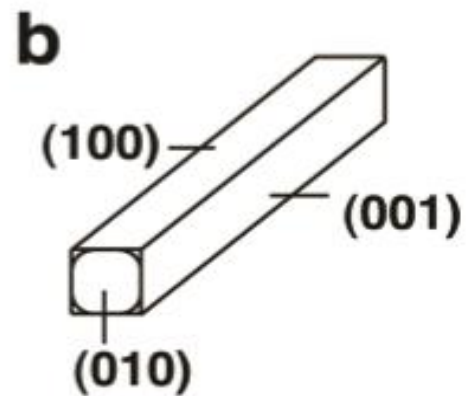
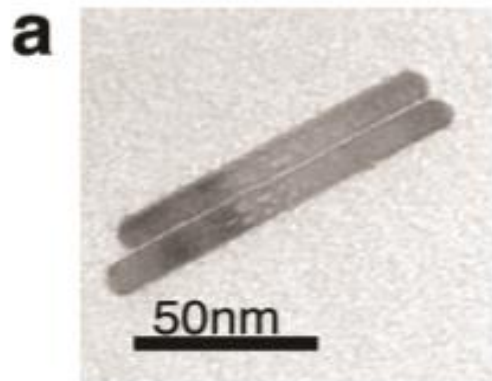


# ADHESION MODELS



Model	Equation
Elovich	$q_t = \left(\frac{1}{\beta}\right) \text{Ln}(1 + \alpha\beta t)$
Simplified Elovich	$q_t = \left(\frac{1}{\beta}\right) \text{Ln}(\alpha\beta t)$
Langmuir	$q_t = q_e \left(\frac{k'_{ad}}{k'_{ad} + k_d}\right) (1 - e^{-(k'_{ad} + k_d)t})$
Avrami	$q_t = q_e [1 - \exp(-k_{av}t)^{n_{av}}]$
Hyperbolic Tangent	$q_t = q_e \left[ \tanh\left(\pi \frac{t}{t_e}\right) \right]^n$
Mixed first and second order	$q_t = q_e \frac{1 - \exp(-kt)}{1 - f_2 \exp(-kt)}$
Mixed first and second order of fractal-type	$q_t = q_e \frac{1 - \exp(-k_{flfs}t^\alpha)}{1 - f_2 \exp(-k_{flfs}t^\alpha)}$
Generalized mixed first and second order of fractal-type	$q_t = q_e \frac{1 - \exp(-k_m \int_0^t t^{-h} C_t dt)}{1 - f_2 \exp(-k_m \int_0^t t^{-h} C_t dt)}$

# Surface hydroxyl groups



Z. Song, Boily, *J. Phys. Chem. C* 115 (2011) 17036

Z. Song, Boily, *J. Phys. Chem. C* 116 (2012) 2303

# Surface hydroxyl groups

(100) face			(010) face		
type of group	site density (sites/nm <sup>2</sup> )	crystallographic Fe–O length (Å)	type of group	site density (sites/nm <sup>2</sup> )	crystallographic Fe–O length (Å)
–O	3.09	1.946	$\eta$ -OH <sub>2</sub>	3.53	1.985 (2.129)
				3.53	1.945 (2.054)
			$\mu$ -O(H)	3.53	2.104, 2.054
				3.53	2.129, 2.070
$\mu$ -O	3.09	1.985	$\mu$ -O	3.53	1.945, 1.977
$\mu_{3,I}$ -O(H)	3.09	2.054, 2.054, 2.104		3.53	1.985, 1.946
$\mu_{3,II}$ -O(H)	3.09	2.129, 2.129, 2.070			
$\mu_{3,I}$ -O	3.09	1.945, 1.945, 1.977			
$\mu_{3,II}$ -O	3.09	1.945, 1.945, 1.977			

Z. Song, Boily, *J. Phys. Chem. C* 115 (2011) 17036

Z. Song, Boily, *J. Phys. Chem. C* 116 (2012) 2303

# MAIN FINDINGS (PART II)

The magnetic hyperfine fields associated to the iron ions located near the chloride vacancies showed small variations with the adsorption of the contaminants.

Akaganeite offers unique properties for the efficient removal of pollutants from aqueous solutions, such as large specific surface area, presence of tunnel sites and ample possibilities of synthesis with modified surfaces.

Among the equations for the adsorption kinetics, the fractal-like types are the ones that better described the data, suggesting the presence of heterogeneous surface adsorption sites in akaganeites.

Synthesis in presence of different cations is an alternative method for modifying morphology, particle size, dimensionality, porosity, crystalline structure, thermal stability and surface properties and to enhance the performance as adsorption of contaminants from water.



UNIVERSIDAD  
DE ANTIOQUIA  
1803



**Thank you**



**International Symposium  
on the Industrial Applications of the Mössbauer Effect**  
Palacký University Olomouc, September 11–16, 2022

## ADSORPTION KINETICS

- Adsorption kinetics describes the adsorption rate of the adsorbate onto the adsorbent and determines the time at which equilibrium is reached.
- There are three stages in the adsorption process: (i) mass transfer (adsorbate) from the solution to the surface of the adsorbent, (ii) diffusion of the adsorbate towards the adsorption sites, and (iii) adhesion of the adsorbate on the surface of the adsorbent.
- Broadly speaking, adsorption kinetic models can be classified as: diffusional or mass transport and adhesion. A third group of models combine diffusion and adhesion.